

Evaluating the Performance of Cross-Directional Control Systems

Stephen R. Duncan[†], Guy A. Dumont[‡] and Dimitry M. Gorinevsky*

[†]Department of Engineering Science, University of Oxford,
Oxford OX1 3PJ, United Kingdom

[‡]Pulp and Paper Centre, University of British Columbia,
2385 East Mall, Vancouver V6T 1Z4 Canada

*Honeywell Technology Center, Honeywell, Cupertino, CA 95014
stephen.duncan@eng.ox.ac.uk

Abstract

Methods have been developed for monitoring the performance of SISO control systems, which compare the variance of the output achieved from the plant to an estimate of the variance that could be achieved by minimum variance control. The methods require knowledge of only the inherent delay within the process. This paper extends these ideas to analyze the performance of cross-directional control systems for sheet processes such as paper machines, which are large multivariable systems. Because such systems are inherently ill-conditioned, the performance is compared against that of a generalized minimum variance controller designed to avoid controlling poorly controllable spatial and dynamic modes. The results of applying the algorithm to data from a paper machine are presented.

1. Introduction

Control systems are designed and tuned to deliver a specified level of performance, generally quantified in the form of the minimization of a performance index. In practice, an important problem is the assessment of the actual performance delivered by a deployed control system. Recent years have witnessed a significant activity towards the development of performance monitoring tools for single-input, single-output (SISO) control systems [1, 2, 3, 4]. Typically, those techniques involve estimating the achievable performance under minimum variance or linear quadratic control and comparing it with the achieved variance. It is remarkable that normal operating data, together with the knowledge of the process time delay, are theoretically sufficient to estimate the minimum achievable variance. In practice, however, minimum variance control results in excessive control effort and poor marginal stability. Therefore a number

of performance monitoring methods have been developed that use a detuned minimum variance controller as benchmark. The extension of performance monitoring techniques to the control of distributed parameter systems, as exemplified by the control of paper machines, has received relatively little attention, despite the practical importance of the problem, with the recent exception of [5, 6]. Because of the significant costs associated with the operation of paper machines, it is important for papermakers to maximize the return on their assets by ensuring that the control systems for basis weight, moisture and caliper are delivering the required performance. This paper presents a method for developing simple and reliable tools for evaluating the performance of an industrial paper machine cross-directional control system.

The main result of this work is a graphical tool for evaluating and tuning the performance of a cross-directional (CD) control system. The tool provides a comparison of the 2-D closed-loop variation patterns achieved by the current controller and that of the "best" performance theoretically achievable. The calculation of the "best" performance assumes that the spatial and dynamic characteristics of both the actuator responses and the disturbances are separable and that the spatial responses of the actuators are known and are spatially invariant. This assumption is reasonable given the proliferation of model-based control packages that include identification tools, independent of CD position, the effect of actuator spatial response CD-dependency being an area on future research. Practical limitations on actuator movement that make minimum-variance control impossible to achieve in practice are accounted for as soft constraints.

Control loop performance monitoring tools developed for SISO control systems do not require knowledge of the plant dynamics apart from the time delay of the

process [1, 2, 3]. In [6], a simple and very approximate measure of CD control performance is derived in total absence of knowledge of the dynamic and spatial responses of the system. In [5], performance measures were derived that assumed perfect knowledge of both dynamic and spatial responses and disturbance characteristics. The method proposed here falls somewhat in between, as it relies on knowledge of the dynamic and spatial responses of the *actuators* acquired during prior identification experiments. However, the characteristics of the *disturbances* will be estimated on-line from operational data.

2. General Methodology

For the purpose of this study, the process can be described by

$$\mathbf{y}_a(t) = q^{-d} \frac{B(q^{-1})}{A(q^{-1})} \mathbf{G} \mathbf{u}_a(t) + \frac{C(q^{-1})}{A(q^{-1})} \mathbf{e}(t) \quad (1)$$

where $\mathbf{y}_a(t) \in R^m$ is a vector consisting of the paper properties measured at m locations (databoxes) across the sheet, $\mathbf{u}_a(t) \in R^n$ is a vector containing the moves applied to the n actuators across the sheet, d is the inherent delay in the system, $\mathbf{G} \in R^{m \times n}$ is the so-called interaction matrix describing the steady-state spatial responses of the actuators and $\mathbf{e}(t) \in R^m$ is a vector containing the disturbances entering the process at each of the m measurement positions. $\mathbf{e}(t)$ is taken to be zero-mean white noise vector with covariance $E[\mathbf{e}(t)\mathbf{e}(t)^T] = \mathbf{\Lambda} \in R^{m \times m}$. The subscript a is used to denote the inputs and outputs achieved by the existing controller on the plant, while the same quantities with subscript o will denote inputs and outputs achievable under generalized minimum variance control. The method developed here relies on the knowledge of $A(q^{-1})$, $B(q^{-1})$, \mathbf{G} and d obtained from prior experiments, using the methods described in [7]. Using these values, a real-time performance assessment of the existing control system is provided by displaying the difference between the achieved measurement profiles and the optimally achievable ones, while accounting for the limiting effect of actuator constraints.

Computing the Optimal Unconstrained Performance. Although it is possible to develop a minimum-variance controller for the controller in (1), this controller is known to be sensitive to modeling errors and to result in control signals of unacceptably large amplitude. Consequently, the optimal controller will be a detuned version of this controller, obtained by the introduction of two parameters ρ and μ (see e.g. [8]) to give

$$\mathbf{u}_o(t) = -\mathbf{K}_o(q^{-1})\mathbf{y}_o(t) \quad (2)$$

where

$$\mathbf{K}_o(q^{-1}) = \frac{H(q^{-1})}{B(q^{-1})F(q^{-1}) + \rho C(q^{-1})} (\mathbf{G}^T \mathbf{G} + \mu \mathbf{I}_n)^{-1} \mathbf{G}^T \quad (3)$$

where $F(q^{-1})$ and $H(q^{-1})$ satisfy

$$C(q^{-1}) = A(q^{-1})F(q^{-1}) + q^{-d}H(q^{-1}) \quad (4)$$

With this controller, the optimal output is

$$\mathbf{y}_o(t) = [\mathbf{I}_m + \mathbf{Q}_o(q^{-1})]^{-1} \frac{C(q^{-1})}{A(q^{-1})} \mathbf{e}(t) \quad (5)$$

where $\mathbf{Q}_o(q^{-1})$ is defined as the open loop transfer function

$$\mathbf{Q}_o(q^{-1}) = g(q^{-1})\mathbf{G}\mathbf{K}_o(q^{-1}) \quad (6)$$

where $g(q^{-1}) = q^{-d}B(q^{-1})/A(q^{-1})$. The aim of the analysis is to express $\mathbf{y}_a(t) - \mathbf{y}_o(t)$, the difference between the output observed on the paper machine and the optimal output from the GMV controller, in terms of $\mathbf{y}_a(t)$ and $\mathbf{u}_a(t)$, both of which are available from the machine. Algebraic manipulations lead to

$$\mathbf{y}_a(t) - \mathbf{y}_o(t) = \mathbf{T}_o(q^{-1})\mathbf{y}_a(t) + \mathbf{S}_o(q^{-1})g(q^{-1})\mathbf{G}\mathbf{u}_a(t) \quad (7)$$

where are $\mathbf{S}_o(q^{-1}) = [\mathbf{I}_m + \mathbf{Q}_o(q^{-1})]^{-1}$ and $\mathbf{T}_o(q^{-1}) = \mathbf{I}_m - \mathbf{S}_o(q^{-1})$ respectively the sensitivity function and complementary sensitivity function for the optimal feedback loop. The CD variation in the observed output and the optimal output can be expressed in terms of the 2σ -measure, commonly used in industry, which are $E\|\mathbf{y}_a(t)\|_2$ and $E\|\mathbf{y}_o(t)\|_2$ respectively.

Because there may be more than 600 measuring positions across the paper machine, both $\mathbf{S}_o(q^{-1})$ and $\mathbf{T}_o(q^{-1})$ can be very large matrices. To simplify the analysis, introduce the singular value decomposition, $\mathbf{G} = \mathbf{U}_1 \mathbf{\Sigma} \mathbf{V}^T$, where $\mathbf{\Sigma} = \text{diag}\{\sigma_i\} \in R^{n \times n}$ is a diagonal matrix containing the n singular values of \mathbf{G} , $\mathbf{V} \in R^{n \times n}$ is the matrix of right singular vectors and $\mathbf{U}_1 \in R^{m \times n}$ contains the first n left singular vectors. Using this decomposition gives

$$\mathbf{G}(\mathbf{G}^T \mathbf{G} + \mu \mathbf{I}_n)^{-1} \mathbf{G}^T = \mathbf{U}_1 \text{diag} \left\{ \frac{\sigma_i^2}{\sigma_i^2 + \mu} \right\} \mathbf{U}_1^T \quad (8)$$

so that $\mathbf{T}_o(q^{-1}) = \mathbf{U}_1 \text{diag}\{p_i(q^{-1})\} \mathbf{U}_1^T$, where

$$p_i(q^{-1}) = \frac{\sigma_i^2 B[C - AF]}{C[\rho(\sigma_i^2 + \mu)A + \sigma_i^2 B] + \mu ABF} \quad (9)$$

and $\mathbf{S}_o(q^{-1})g(q^{-1})\mathbf{G} = \mathbf{U}_1 \text{diag}\{r_i(q^{-1})\} \mathbf{V}^T$ where

$$r_i(q^{-1}) = q^{-d} \frac{B}{A} [1 - p_i(q^{-1})] \quad (10)$$

Since $A(q^{-1})$, $B(q^{-1})$, d and \mathbf{G} are available from a previous identification experiment [7], the computation of (9) and (10) requires the estimation of both $F(q^{-1})$ and $C(q^{-1})$.

Estimating the $F(q^{-1})$ -polynomial The assumption that the spatial and dynamic responses of both the actuators and the disturbances are separable, allows the dynamics of the process to be described in terms of scalar polynomials. Because MD control is typically done at a rate of once a scan (although industrial systems are capable of MD control two or three times per scan), MD-aggregated data will be used to estimate $F(q^{-1})$. If $\bar{y}_a(t)$ and $\bar{u}_a(t)$ denote the average measurement and control settings across the sheet the estimate of $F(q^{-1})$ relies on the fact that for a process modeled by

$$\bar{y}_a(t) = q^{-d} \frac{B(q^{-1})}{A(q^{-1})} \bar{u}(t) + \frac{C(q^{-1})}{A(q^{-1})} \bar{e}(t) \quad (11)$$

under a general feedback controller of the form

$$\bar{u}(t) = -\frac{N(q^{-1})}{D(q^{-1})} \bar{y}(t) \quad (12)$$

then the closed-loop system can be expressed as

$$\bar{y}_a = F\bar{e} + q^{-d} \frac{HD - BFN}{AD + q^{-d}BN} \bar{e} \quad (13)$$

with $\deg F = d - 1$. Thus, it is only necessary to identify the output of the process as a time-series and to compute the first d Markov parameters to find $F(q^{-1})$. Here, the time series used to represent the closed-loop system is modelled as white noise \bar{e} filtered through a Laguerre network [3]

$$\begin{aligned} \mathbf{l}(t+1) &= \mathbf{A}\mathbf{l}(t) + \mathbf{b}\bar{e}(t) \\ \bar{y}_a(t) &= \mathbf{c}^T \mathbf{l}(t) + \bar{e}(t) \end{aligned} \quad (14)$$

where \mathbf{l} is the state vector composed of the outputs of the Laguerre filters, \bar{e} is zero-mean white noise, \mathbf{A} and \mathbf{b} are respectively a $N \times N$ matrix and a vector of dimension N characterizing the Laguerre network, and whose terms only depend on the pole of those filters and the sampling interval and \mathbf{c} is a vector of dimension N containing the Laguerre spectrum of the time series being modelled. Typically a network with $N = 10$ filters is used. The vector \mathbf{c} is easily estimated from closed-loop data, and the coefficients of $F(q^{-1})$ are obtained from

$$f_0 = 1, \quad f_1 = \mathbf{c}^T \mathbf{b}, \quad f_2 = \mathbf{c}^T \mathbf{A} \mathbf{b}, \quad f_3 = \mathbf{c}^T \mathbf{A}^2 \mathbf{b}, \dots \quad (15)$$

Estimating the $C(q^{-1})$ -polynomial To estimate the disturbance characteristics, i.e. the $C(q^{-1})$ -filter, the MD-aggregated model in (11) is written as

$$w(t) = A(q^{-1})\bar{y}_a(t) - q^{-d}B(q^{-1})\bar{u}_a(t) = C(q^{-1})\bar{e}(t) \quad (16)$$

Because $A(q^{-1})$, $B(q^{-1})$ and d are assumed known, it is straightforward to generate the sequence $w(t)$. $C(q^{-1})$ can be estimated using a simple extended least-squares algorithm. Typically, $C(q^{-1})$ will be restricted to a first or second-order polynomial.

3. Implementation

The data is presented to the algorithm in the form of measurements taken from a scanning gauge and the settings of actuators at the end of each scan. The algorithms corresponding to the above derivations were implemented in MATLAB. The algorithm generates a contour plot or color image of the squared difference between the actual and optimal variability for a moving window of 50 scans. The results are updated at the end of each scan. As described in the next section, the algorithm was used to analyze the performance of one paper machine that had over 600 measurement positions across the sheet and 235 actuators, so some of the matrices used in the calculations were extremely large. The algorithm needed to be implemented carefully to avoid excessive computational load. The major computational burden is the calculation of the singular value decomposition of the interaction matrix, \mathbf{G} . However, \mathbf{G} is obtained from a separate identification experiment and in the current implementation of the algorithm, \mathbf{G} is not updated online. As a result, the singular value decomposition forms part of the setup procedure for the algorithm and could, if necessary, be performed offline. Once the singular value decomposition has been performed, the online processing can be simplified by defining $\tilde{\mathbf{y}}_a(t) \in R^n$ and $\tilde{\mathbf{u}}_a(t) \in R^n$ as

$$\tilde{\mathbf{y}}_a(t) = \mathbf{U}_1^T \mathbf{y}_a(t) \quad \tilde{\mathbf{u}}_a(t) = \mathbf{V}^T \mathbf{u}_a(t) \quad (17)$$

The columns of \mathbf{U}_1 span the controllable subspace of the interaction matrix, \mathbf{G} , so $\tilde{\mathbf{y}}_a(t)$ contains the spatial components of $\mathbf{y}_a(t)$ that can be controlled by the actuators [9]. Given that $\mathbf{U}_1^T \mathbf{U}_1 = \mathbf{I}_n$, then the expression for the difference between the observed output and the optimal output in (7) can be expressed as

$$\tilde{\mathbf{y}}_a(t) - \tilde{\mathbf{y}}_o(t) = \text{diag}\{p_i(q^{-1})\} \tilde{\mathbf{y}}_a(t) + \text{diag}\{r_i(q^{-1})\} \tilde{\mathbf{u}}_a(t) \quad (18)$$

In this form, when the $F(q^{-1})$ and $C(q^{-1})$ polynomials are estimated at the end of each scan, the problem of generating $\tilde{\mathbf{y}}_a(t) - \tilde{\mathbf{y}}_o(t)$ has been reduced to a set of n SISO filters, one for each controllable mode. Transforming the problem into the controllable subspace decouples the individual modes and reduces the computational and storage requirements of the algorithm. To display the results, $\mathbf{y}_a(t) - \mathbf{y}_o(t)$ can be recovered using $\mathbf{y}_a(t) - \mathbf{y}_o(t) = \mathbf{U}_1 [\tilde{\mathbf{y}}_a(t) - \tilde{\mathbf{y}}_o(t)]$. Note that only the controllable components of $\mathbf{y}_a(t) - \mathbf{y}_o(t)$, spanned by the columns of \mathbf{U}_1 are being reconstructed. Because both $\mathbf{y}_a(t)$ and $\mathbf{y}_o(t)$ contain the same uncontrollable components, there will be no uncontrollable components in $\mathbf{y}_a(t) - \mathbf{y}_o(t)$. In essence, the analysis determines the portion of the disturbance lying *within the controllable subspace* that could be removed by the optimal controller, and is not removed by the existing controller.

It is sometimes useful to display the "mapped" error profile $\mathbf{G}^T[\mathbf{y}_a(t) - \mathbf{y}_o(t)]$, which allows regions of poor control to be associated with individual actuators. This can be generated directly from

$$\mathbf{G}^T[\mathbf{y}_a(t) - \mathbf{y}_o(t)] = \mathbf{V}\Sigma(\tilde{\mathbf{y}}_a(t) - \tilde{\mathbf{y}}_o(t)) \quad (19)$$

4. Results

The procedure described above was tested on data from a number of paper machines. The results presented here are from a data set consisting of 100 scans of basis weight measurements taken at 660 databoxes across the sheet controlled by 235 actuators on a dilution flow headbox. The process was operating in closed loop with an industrial controller. No information about the controller was used for the analysis. Prior identification performed on the open-loop system was used to determine the process model. The analysis has been carried out using $\mu = 0.001$ and $\rho = 0.1$. Figure 1 shows a contour plot of the squared deviation from optimality over 50 scans (expressed in the form $\mathbf{G}^T[\mathbf{y}_a(t) - \mathbf{y}_o(t)]$) and it can be seen that there are a number of "streaks" of relatively poor control, particularly in the vicinity of actuators 122 and 194. Figure 2 compares the average cross-directional profile that the remains in the sheet after the optimal control is applied (solid line) and the corresponding profile observed on the machine (dashed line). Using the conventional 2σ -measure, for the actual CD profile, $2\sigma = 0.025$, while the optimal CD profile, $2\sigma = 0.017$, which corresponds to a reduction of about 33%. In addition, the ratio of actual MD variance to optimal MD variance is about 2.5, indicating that the existing controller is conservatively tuned.

The results show that the difference between the CD profiles of measured output and the optimal output tends to occur in the higher order spatial modes, suggesting that the controller implemented on the plant has been detuned so that it does not respond to higher order modes. This is to be expected for two main reasons. Firstly, control of higher order modes requires large actuator inputs [10, 11], which can violate constraints on the magnitude of the inputs. Secondly, the controller is most sensitive to uncertainties in the higher order modes [12], so practical controllers are often detuned so that they do not respond to these modes, in order to make the control system robust.

5. Handling Constraints

The calculation of the output from the optimal controller has not considered any constraints on the inputs applied to the actuators. As the results of the previous section have demonstrated, this means that

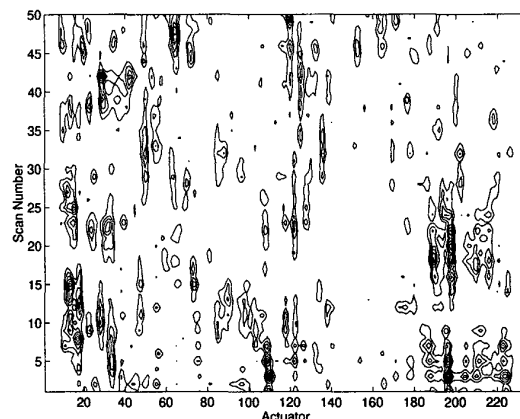


Figure 1: Contour plot of squared deviation between residual variation observed on the paper machine and the residual variation from the optimal controller in (3)

the major discrepancy between the measured and optimal outputs occurs in the higher order spatial modes. In practice, the most common form of constraints restricts the magnitude of the actuator inputs, which can be expressed in the form [13]

$$\|\mathbf{u}(t)\|_\infty \leq \mathbf{u}_{max} \quad (20)$$

The determination of the optimal inputs in the presence of constraints requires the solution of a quadratic programme at each time step [14, 13], which is not appropriate for an online implementation of a monitoring system. However, actuator limits can be accommodated by soft constraints, by using $\|\mathbf{u}(t)\|_\infty \leq \|\mathbf{u}(t)\|_2$ and choosing the weighting parameters, μ and ρ , to ensure that $\|\mathbf{u}(t)\|_2 \leq \mathbf{u}_{max}$. To do this, note that

$$\mathbf{u}_o(t) = -\mathbf{K}_o(q^{-1})[\mathbf{I}_m + \mathbf{Q}(q^{-1})]^{-1}(\mathbf{y}_a(t) - \mathbf{g}(q^{-1})\mathbf{G}\mathbf{u}_a(t)) \quad (21)$$

From the previous analysis, $\mathbf{K}_o(q^{-1})[\mathbf{I}_m + \mathbf{Q}(q^{-1})]^{-1}$ can be written as $\mathbf{V}\text{diag}\{m_i(q^{-1})\}\mathbf{U}_1^T$ where

$$m_i(q^{-1}) = \frac{\sigma_i^2 AH}{C[\rho(\sigma_i^2 + \mu)A + \sigma_i^2 B] + \mu ABF} \quad (22)$$

so $\|\mathbf{u}_o(t)\|_2$ becomes

$$\|\text{diag}\{m_i(q^{-1})\}\tilde{\mathbf{y}}_a(t) + \text{diag}\{g(q^{-1})\sigma_i m_i(q^{-1})\}\tilde{\mathbf{u}}_a(t)\|_2 \quad (23)$$

where $\tilde{\mathbf{y}}_a(t)$ and $\tilde{\mathbf{u}}_a(t)$ are defined in (17). Given that past values of $\tilde{\mathbf{y}}_a(t)$ and $\tilde{\mathbf{u}}_a(t)$ are stored as part of the algorithm, when new estimates of $F(q^{-1})$ and $C(q^{-1})$ are determined at each time step, values of μ and/or ρ can be chosen automatically to ensure that the right hand side of (23) does not exceed \mathbf{u}_{max} .

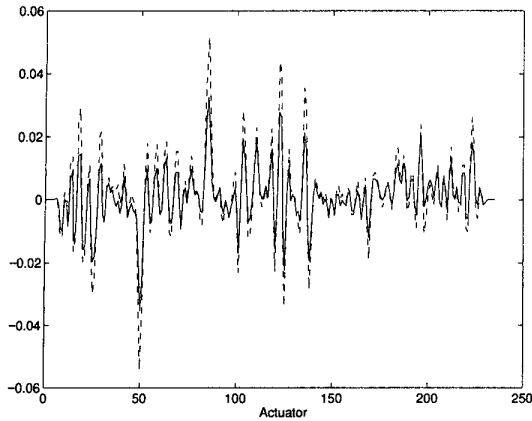


Figure 2: Plot of average profile of CD basis weight variations observed on machine (dashed line) and optimal CD profile (solid line)

6. Conclusions

This paper has described a performance assessment algorithm for CD profile control systems. The algorithm that takes profiles of CD variations from the process and combines them with the actuator settings to determine the difference between the actual level of variation observed on the sheet and an estimate of the level of variation that could be achieved using a GMV controller. This allows performance indices for both CD and MD variations to be calculated. The algorithm has been tested on real-life data from a system for controlling basis weight variations on a paper machine, using a dilution headbox. As expected, the results show that the existing control system is unable to remove all of the higher order spatial modes, in particular due to the constraints on the inputs. Although the algorithm cannot accommodate strict input constraints, a method is proposed which replaces them by soft constraints. Current developments are investigating ways of tackling more general constraints and taking better advantage of redundant information contained in the estimates of $F(q^{-1})$ and $C(q^{-1})$.

Acknowledgements

This work was supported by Honeywell-Measurex with the help of NRC IRAP Grant RDA312886. The first author gratefully acknowledges financial support from the UK Royal Academy of Engineering as part of an Engineering Foresight award and the British Columbia Advanced Systems Institute while on leave at the UBC Pulp and Paper Centre.

References

- [1] T.J. Harris, "Assessment of control loop performance," *Canadian Journal of Chemical Engineering*, vol. 67, pp. 856–861, 1989.
- [2] L.D. Desborough and T.J. Harris, "Performance assessment measures for univariate feedback control," *Canadian Journal of Chemical Engineering*, vol. 70, pp. 1186–1197, 1992.
- [3] C.B. Lynch and G.A. Dumont, "Control loop performance monitoring," *IEEE Trans Control Systems Technology*, vol. 4, pp. 185–192, 1996.
- [4] L.C. Kammer, R.R. Bitmead, and P.L. Bartlett, "Optimal controller properties from closed-loop experiments," *Automatica*, vol. 34, pp. 83–91, 1998.
- [5] C. Fu, S. Nuyan, and S. Bale, "CD control performance assessment," in *Proc. Control Systems '98*, Porvoo, Finland, 1998.
- [6] Z. Nestic, M.S. Davies, G.A. Dumont, S. McLeod, and I. Shaw, "Paper machine operator reel/roll display for improved paper quality," in *Proc. Control Systems '98*, Porvoo, Finland, 1998.
- [7] D. Gorinevsky, M. Heaven, and C. Gheorge, "High-performance identification of cross-directional processes," in *Proc. Control Systems '98*, Porvoo, Finland, 1998, pp. 347–354.
- [8] S.R. Duncan and K.W. Corscadden, "Mini-max control of cross-direction variations on a paper machine," *IEE Proceedings on Control Theory and Applications*, vol. 145, no. 2, pp. 189–196, 1998.
- [9] S.R. Duncan, "The cross-directional control of web forming processes," PhD thesis, University of London, London, UK, 1989.
- [10] S.R. Duncan and G.F. Bryant, "Spatial controllability of cross-directional control systems for web processes," *Automatica*, vol. 33, no. 2, pp. 139–153, 1997.
- [11] G.E. Stewart, G.A. Dumont, and D.M. Gorinevsky, "Robust GMV cross directional control of paper machines," in *Proc. American Control Conf.*, Philadelphia, PA, 1998, pp. 3002–3007.
- [12] A.P. Featherstone and R.D. Braatz, "Integrated robust identification and control of large scale processes," in *Proc. American Control Conf.*, Philadelphia, PA, 1998.
- [13] W.P. Heath, "Orthogonal functions for cross-directional control of web forming processes," *Automatica*, vol. 32, no. 2, pp. 183–198, 1995.
- [14] S.-C. Chen, R.M. Snyder, and R.G. Wilhelm, "Adaptive profile control for sheetmaking processes," in *Proc. 6th IFAC/IMEKO Conf. on Instrumentation and Automation in the Paper, Rubber, Plastics and Polymerisation Industries (PRP 6)*, Akron, OH, 1986, pp. 77–83.